Journal of Applied Electrochemistry (2005) 35:1111–1120
DOI 10.1007/s10800-005-9005-y

Development of high-capacity primary alkaline manganese dioxide/zinc cells consisting of Bi-doping of MnO_2

DEYANG QU[1,*], DONALD DIEHL[2,4], B.E. CONWAY[3], W.G. PELL[3] and S.Y. QIAN[3]
[1]*Department of Chemistry, University of Massachusetts Boston, 100 Morrissey Blvd., Boston, MA 02125-3393,*
[2]*Emtech, 2486 Dunwin Dr., Mississauga, ON, Canada*
[3]*Department of Chemistry, University of Ottawa, Ottawa, ON, Canada K1N 6N5*
[4]*Component Concepts, 2016 Salinente Way, Carlsbad, CA 92009, USA*
*(*author for correspondence, tel.: +781-287-6035; e-mail: deyang.qu@UMB.edu)*

Received 12 January 2004; accepted in revised form 20 June 2005

Key words: Bi-doping, manganese dioxide, primary alkaline cell

Abstract

The feasibility of using Bi-doped manganese dioxide as the cathode in a primary alkaline zinc cell is discussed. A Bi-doped MnO_2 cathode material made by the CMD process is examined with respect not only to its discharge in conditioning cycles but also with achievement of practically high voltage on discharge. With suitable composition of the Bi/MnO_2 composite, remarkably high C-rates for discharge and recharge are achieved with little polarization. The Bi–Mn–O compounds with possible structures are also discussed.

1. Introduction

In the current technology of making primary MnO_2/Zn cells, including Léclanché and alkaline types, γ-MnO_2, e.g. Electrolytic Manganese Dioxide (EMD) or Chemical Manganese Dioxide (CMD) is used as the active cathode material. Intrinsically, γ-MnO_2 can only release one of its two available redox electrons at a practically useable potential and at a practically appreciable discharge rate. The second electron is only released at a useless low potential and at impractically low rate [1]. The theoretical capacity of EMD is 308 mA g^{-1}.

The electrochemical science and technology of zinc chemistry is quite mature, even though good engineering work has still to be done to prevent Zn from premature passivation. Both of the two electrons of the Zn anode can be utilized almost reversibly in the alkaline cell. Thus, in order to improve the capacity of alkaline MnO_2/Zn cells, the discharge capacity and rate capability of the MnO_2 cathode must be improved, especially to provide use of the second electron of that material upon reduction.

A general mechanism for the reduction of regular MnO_2 was proposed by Kozawa and Powers [2–5] in terms of a so-called first homogeneous stage in which e^- and proton injection takes place into the MnO_2 lattice and is partially reversible over a restricted number of cycles conducted over the 1 e^- reduction potential range, followed by a second-electron reduction stage that is irreversible except when the MnO_2 has been doped by Bi species (Wroblowa and co-workers [6, 7], see below).

In order to develop a high-capacity MnO_2 material that can deliver close to 2 e^- capacity during its discharge, attempts have been made to dope the MnO_2 with foreign cations. Many elements in the Periodic Table, except those that are radioactive, have been tried [8], but only Bi(III) and Pb(II) discovered independently by researchers from Hitachi [9] and by Wroblowa and co-workers from Ford Motor company [6, 7] in the1980's, can facilitate the two-electron reduction of MnO_2. The mechanism of the Bi-induced, 2-electron reduction has been studied in depth by Conway's research group [10–14]. An heterogeneous reduction mechanism involving soluble $Mn(OH)_4^-$ species was proposed and Bi(III) was believed to act as a catalyst which could reduce the energy barrier for reductive transfer of the second electron; thus not only is the reduction overpotential reduced, but also the kinetics of charge-transfer are correspondingly improved for the reduction involving the second electron. In addition, unlike the behavior of conventional EMD, Bi and Pb dopants also allow the manganese dioxide to maintain significant rechargeability even from large (ca. 90%) depths of discharge.

However, the Bi-doped manganese dioxide reported by Wroblowa [6, 7], made by both chemical and physical modifications cannot deliver its 2-electron capacity during the very first discharge, but only after significant formation cycles. This characteristic has impeded the

use of Bi-doped MnO_2 as cathode material in primary alkaline cells. Another significant obstacle for use of Bi-doped MnO_2 has been its low discharge voltage against the Zn anode. Even though Bi-doped manganese dioxide can tolerate very high discharge current-densities [7], most of the flat, second-electron discharge voltage is barely at −0.4 V vs Hg/HgO, which is close to 0.9 V in alkaline cells, taking into consideration the overpotential of the Zn anode during discharge. In order to utilize the doped MnO_2 in primary cells and to take the advantage of the currently unused second electron, these two obstacles have to be overcome.

2. Experimental

2.1. *Instrumental details and electrochemical cell*

Constant current "galvanostatic" discharges were conducted by means of a Solartron Electrochemical Interface 1278 for the half-cell discharge and by a Maccor system for the discharge of AA size test cells. Unless otherwise specified, an Hg/HgO/KOH reference electrode was used in the half-cell tests and the AA cell voltage was that recorded against the Zn anode. X-ray powder diffraction patterns of the MnO_2 materials were collected using a Siemens (now Bruker AXS) D5000 powder diffractometer equipped with a Cu target X-ray tube and monochromator.

2.2. *Synthesis of Bi-doped MnO_2 material*

2.2.1. *Chemical-Modified (CM) manganese dioxide*

The CM MnO_2 material was synthesized based on the procedures reported in Ford patent [16]. The Bi-doped MnO_2 was made by co-precipitation. $Mn(NO_3)_2$ was mixed with $Bi(NO_3)_3$ in acidic solution at desired Mn/Bi mole ratio. After adding KOH, the hydroxide was precipitated. The suspension of the hydroxide was then chilled in an ice bath and subjected to treatment by a steam of O_2 to form bismuth birnessite compound, $Bi_xMn_yO_{2y+1.5x}$. $0.5yH_2O$, where the ratio y/x is 14 in the present case.

2.2.2. *CM manganese dioxide with further oxidation*

In order to bring the oxidation state of Mn close to 4+, CM MnO_2 synthesized according to the procedures in Section 2.2.1 was thermally treated in a tube furnace at 150 °C overnight with a stream of O_2 passing through.

2.2.3. *Bi-doped manganese dioxide made with CMD method*

The CMD Bi-MnO_2 material was synthesized according to the example 4 in Duracell patent [21] with the following exceptions:

1. $Bi(NO_3)_3$ was added.
2. the particle size of Kerr-McGee EMD, which was used as seeds for the precipitation, were less than 10 μm.
3. After the product was cooled to room temperature, instead of rinsing with distilled water, the pH of the solution was adjusted to 10 by adding NaOH.

In details $MnSO_4 \cdot 4H_2O$ was dissolved with stoichiometric amount of $Na_2S_2O_8$ in distilled water. $Bi(NO_3)_3$ was added to the solution, the mole ratio of Mn and Bi was 14. H_2SO_4 may be added, if milky precipitates were formed, the solution should be clear and pinkish. Milled Kerr-McGee EMD with particle size less than 10 μm was added at 1:1 mole ratio of MnO_2 and $MnSO_4$. The mixture solution was then heated to 55, 75 and 100 °C, subsequently as mentioned in the patent [21], before it was cooled to room temperature. The pH of the mixture was adjusted to 10 by adding 2 M NaOH solution while stirring. The product was then filtrated, washed 3 times with distilled water and vacuum dried at 100 °C for 5 h.

2.3. *Construction of MnO_2 electrodes and electrochemical half-cells*

Detailed descriptions of the electrode construction and the electrochemical cell were reported previously [15]. Unless otherwise specified, the MnO_2 electrode was made with the test MnO_2 and Lonza (now Timcal) KS6 graphite at a 9:1 weight ratio with 0.5 wt% Teflon (dry material) being used as binder. The components were thoroughly mixed with a high-speed mixer. The resulting mix was weighed and pressed to form a tablet 22.0 ± 0.2 mm in diameter and 1.8 ± 0.2 in thickness. A two-compartment testing cell was used. The working electrode and the Ni counter-electrode were restrictively housed in the separate compartments which were linked by an electrolyte bridge. Spring pressure was applied to ensure good Ohmic contact between the working electrode tablet and the Ni current-collector. The Hg/HgO reference electrode was electrolytically connected to the working electrode compartment through a Luggin capillary in the usual way.

The MnO_2 material used in the experiments for testing rate capability was Chemically Modified (CM) MnO_2 prepared according to the Ford method [16]. The test electrode was made by mixing CM MnO_2 and KS6 at a 1:10 weight ratio, with an additional 5 wt% Teflon (dry material) being added as binder. The thoroughly mixed composite was then rolled to form a film which was subsequently compressed on a Ni mesh to form the positive electrode.

2.4. *Construction of AA MnO_2/Zn test cells*

Commercial cylindrical alkaline Manganese Dioxide–Zinc cells are made in the bobbin design. Even though cylindrical alkaline MnO_2/Zn cells have been at this stage of mass production for decades, the detailed engineering aspects of making the cells are hardly reported in the scientific and engineering journals. Figure 1 [17] shows the cross-section of a typical cylindrical alkaline cell. The components are housed in a metal can (6 in Figure 1), which is normally made with

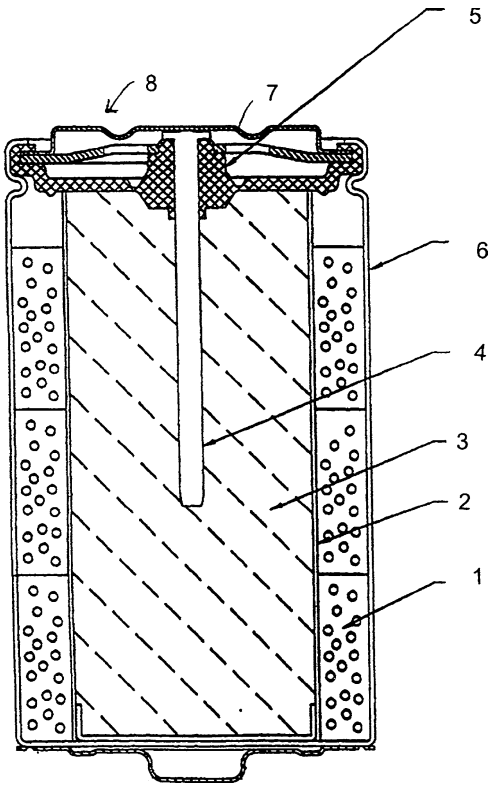

Fig. 1. The configuration of an alkaline cylindrical cell.

Ni-plated steel and the can also serves as the cathode current collector. The cathode (1) contains MnO_2 as electrochemically active cathode reagent, employing graphite as a conductive filler and KOH solution as electrolyte, together with other additives. The cathode is made to have an intimate contact with the metal can to ensure low Ohmic resistivity. Zn gel serves as the anode reagent (3) which is made by suspending Zn particles in gelling agents. Since Zn amalgams are no longer allowed for environmental reasons, inorganic and organic inhibitors are added in the gel to increase the hydrogen evolution overpotential and minimize Zn corrosion and passivation. Studies on the Zn anode will be reported separately. The current collector for the Zn anode is a plated brass nail (4). A non-woven separator (2) is placed between the cathode and anode. A vent mechanism (5), which is designed to burst at a pre-set pressure, is provided as a safety measure in the event of significant internal pressure build-up, and is engineered in the top assembly (7, 8). The cell is then crimp-sealed.

There are two ways of making the MnO_2 cathode electrode: one is to mould the cathode inside the can through impaction, in which process, the cathode mix is fed into the can before impaction takes place, and thus a single-piece cathode is formed inside the metal can. The second way of making the cathode for alkaline MnO_2/Zn cells is to mould the cathode ring first with the rings being subsequently inserted into the can. Ring insertion is either a "slip fit", in which process the ring outer-diameter (OD) is made slightly larger than the can inner-diameter (ID); the cathode ring is then pressed into the can to ensure good can/cathode contact; or the ring insertion is a "drop fit", in which the cathode OD is made slightly smaller than the can ID, so the ring can be "dropped" into the can. A subsequent compaction is then needed to generate intimate can/cathode contact. In the work reported in this paper, alkaline AA-size cells were made using the "slip fit" procedure.

The dies and processes for the cathode moulding and insertion are illustrated in Figure 2. The procedures for pressing the pellets and subsequently moving them directly into the can (slip fit) are listed as follows:

1. Assemble the base, rod and collar as shown in Figure 2.
2. Weigh out the cathode mix for one pellet. One AA cell contains four pellets. Fill the cavity of the die with the mix.

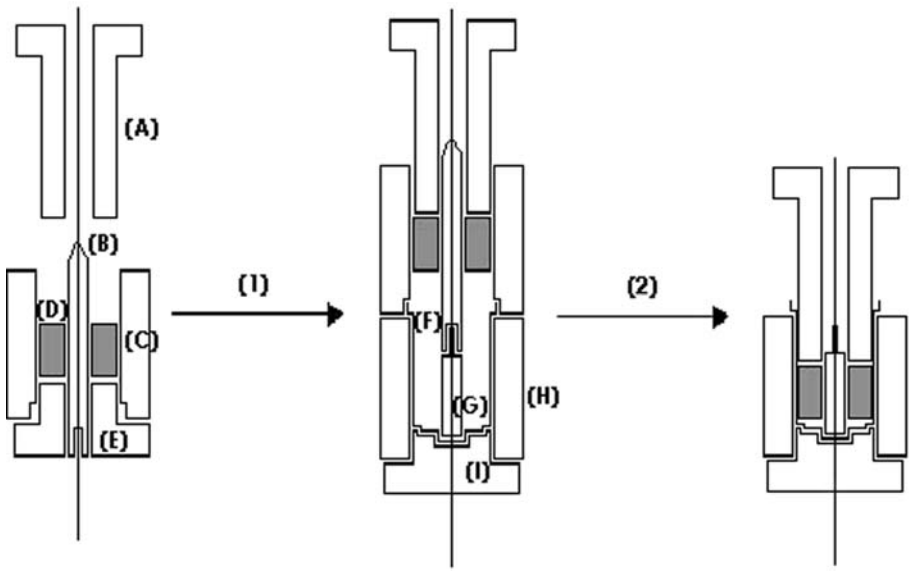

Fig. 2. Diagram for the process of making bobbin-type cylindrical cells: (A) punch; (B) rod; (C) collar; (D) cathode pellet; (E) base; (F) step-can; (G) guide with stud; (H) lower collar; (I) cap.

3. Insert the punch, as shown at the top of Figure 2 into the cavity. Press on a Carver press. A pressure was of about 4000 kg cm^{-2} is used to compact the pellet. Hold the pressure for about 1 min.
4. Remove the base (e in Figure 2) from the assembly. Assemble the cap and lower collar, and place a fresh can in the cavity. Place the guide (G) down into the can (The guide had an 8–32 stud about 1 inch in length screwed into it).
5. Rest the collar assembly on the top of the can as shown in Figure 2. Make sure that the hole in the bottom of the rod mates with the stud in the guide.
6. Place the assembly on the Carver press, depress the punch and push the pellet into the can.
7. Repeat steps (1)–(6) for the remaining 3 pellets.
8. Put pressure on the cathode as shown in Figure 2, using the Carver press, until the required cathode height is reached.

The outer diameter of the cathode pellet was made larger than the inner diameter of the can, so the cathode can be pushed to fit into the can as shown in Figure 2, together using step (8) to ensure a good contact between cathode pellets and the can.

A non-woven separator was placed into the cathode cavity. The cell was pre-wetted by 35 wt% aqueous KOH solution in vacuum. Zn gel recovered from Duracell® D-size cells was used as the anode material. A roof repair tar was used as sealant. The whole cell was then crimp-sealed.

Figure 3 shows a comparison between the discharge curves of an Eveready AA cell, bought from the open-market, and an AA cell made in-house using the above procedures with Kerr-McGee EMD. The cells were discharged through a 5 ohm constant load. This clearly demonstrated the validity of the AA cell fabrication techniques.

3. Results and discussion

3.1. *Bi-doped manganese dioxide material*

Figure 4 shows a comparison of the discharge curves for the three types of Bi-doped MnO_2 synthesized in different ways. The curve (a) in Figure 4 shows the first discharge curve of CM Bi-doped MnO_2 made by chemical modification through the co-deposition process. The resulting low discharge potential and capacity were believed to be due to insufficient oxidation in the air-bubbling stage (e.g. Ref. 16). The average oxidation state of Mn may remain less than 4+. The same doped MnO_2 (Birnessitte in structure) was then subjected to further oxidation by passing pure oxygen gas through the sample at elevated temperature in a tube furnace to bring the oxidation state of Mn close to 4+. In Figure 4, the discharge curve (b) of such Bi-doped MnO_2, subjected to oxidation in pure oxygen at 150 °C for 10 h, is plotted in comparison with that of the non-oxidized Bi-doped MnO_2 (curve a). It is obvious that the further-oxidized Bi-doped MnO_2 manifested much higher discharge potentials on the first discharge, as well as substantially higher discharge capacity. Curve (c) represents the discharge curve of Bi-doped MnO_2 made with CMD method, which will be discussed in detail in Section 3.3.

In the practical application of the alkaline cell, high operating voltage is of equal importance to high total capacity, due to cut-off voltage requirements of many devices. The low discharge voltage of the Bi-doped manganese dioxide compared with EMD is due to the fact that its structure is still Birnessitte. In order to make the Bi-doped MnO_2 a practical cathode material, the operating voltage of the material, at least the voltage for the reductive use of the first electron, has to be as close as possible to that of EMD, while maintaining the

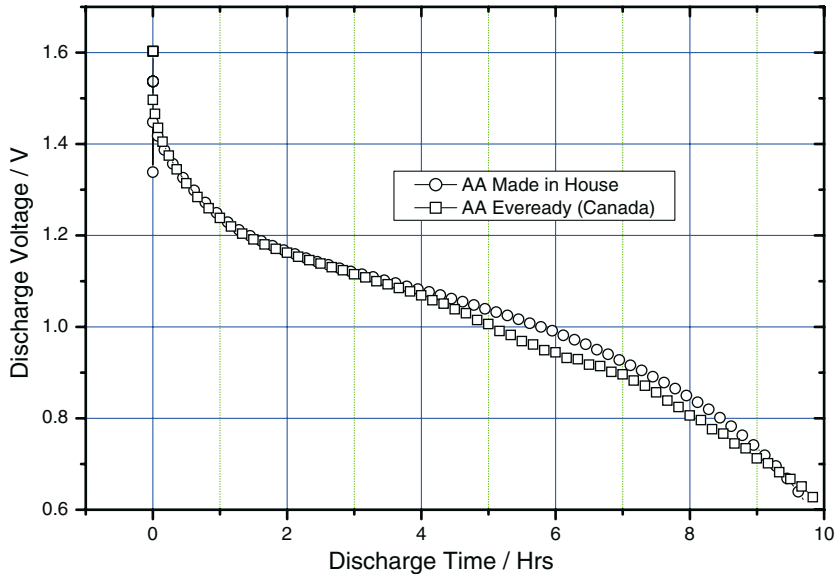

Fig. 3. Comparison of the discharge curves for an Eveready AA primary MnO_2/Zn AA primary MnO_2/Zn cell bought in the open market with the home-made AA cell using Kerr-McGee EMD. The cells were discharged through a 5 ohm constant load.

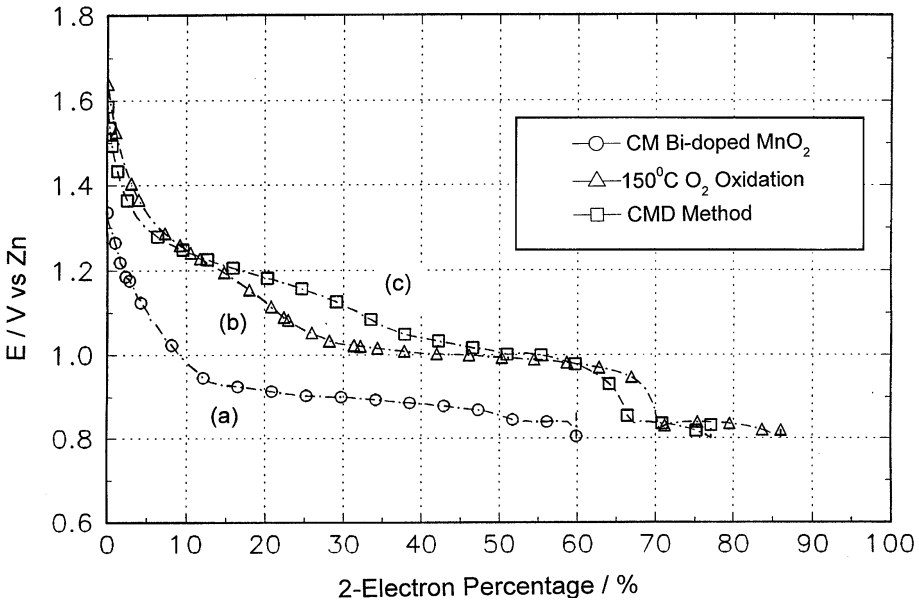

Fig. 4. Comparison of the discharge curves for the Bi-doped MnO_2 electrode made by (a) the co-deposition method; (b) the material made by the co-deposition method being further oxidized in pure O_2 at 150 °C; (c) CMD method. The discharge rate was 30.8 mA g^{-1}.

unique feature of the extended and reversible utilization of the "second electron" of the MnO_2. The mechanism of the 2-electron reduction has been studied in great detail [10, 13], for example the Bi acts as a catalyst to reduce the energy barrier or overpotential for the reduction in the second-electron stage. It is a thermodynamic aspect that the potential for the reduction of the Biressitte MnO_2 is below 1.2 V vs the Zn reference electrode in alkaline solution. Thus it is essential to make the Bi-doped MnO_2 have the same γ-structure as that of EMD, which has been proven to exhibit a high discharge potential for the reduction involving the first electron [1].

In the light of the previous observations, several different methods for the synthesis of Bi-doped manganese dioxide material could lead to Bi-doped γ-MnO_2:

1. Use of the electrolytic method with addition of a suitable Bi compound in the bath [18].
2. Use of the Chemical Manganese Dioxide (CMD) process with addition of EMD as seeds and Bi as dopant.
3. Physical modification by mixing Bi_2O_3 with EMD.

Making Bi-doped manganese dioxide by the electrolytic method has been described [18, 19]; Castledine and Conway [18] investigated, in detail, the mechanism of Bi incorporation by the electrolytic method using H_2SO_4 solution. They suggested that the deposition of bismuth during the production of electrolytic MnO_2, may not be caused directly by the electrolysis, since the potential used for the electrodeposition of MnO_2 lies well above the reversible potential for the Bi^{3+}/Bi couple, but well below that for the Bi^{5+}/Bi^{3+} couple. The bismuth compounds that became included in the EMD were determined to be either $Bi_2(SO_4)_3$ or $BiH(SO_4)_2$. The precipitation was believed to be caused by an increase of local acidity produced by the MnO_2 deposition reaction, which can result in a protonation reaction occurring with subsequent precipitation of bismuth species. In this case, the bismuth compound became incorporated in the matrix of manganese dioxide as sulphate compounds, rather than being occluded into the crystal structure of the MnO_2. In other words, the resulting product can be considered as MnO_2 modified physically at the molecular level, since Bi stays in a separate phase with the MnO_2. As a result, the first discharge of the Bi-doped electrolytic manganese dioxide is similar to that of regular EMD [19] so that the two-electron capacity can only be realized after several conditioning cycles.

3.2. *High charge/discharge capacities of Bi-doped MnO_2*

Figure 5 shows the constant-current charge and discharge curves for CM MnO_2 at various rates. Figure 5a and b show the plots of E vs time and E vs capacity, respectively, for the same set of data. A high percentage of graphite was used to minimize the internal Ohmic resistance for the porous electrode, so the true kinetic aspects of discharge of Bi-doped MnO_2 can be investigated without interference by other parameters.

Figure 5a demonstrates that Bi-doped MnO_2 is capable of being charged and discharged at very high current-density up to a 10C rate (6 A g^{-1}). In addition, the charge/discharge profiles of the Bi-doped MnO_2 electrode are almost independent of the charge/discharge rate. This is an important characteristic of CM MnO_2 that demonstrates the capability of CM MnO_2 being charged/discharged at extremely high rate with little Faradaic polarization. This makes Bi-doped MnO_2 substantially different in behavior from the other types of MnO_2 [11], the discharge profiles of which are very much dependent on the discharge rate.

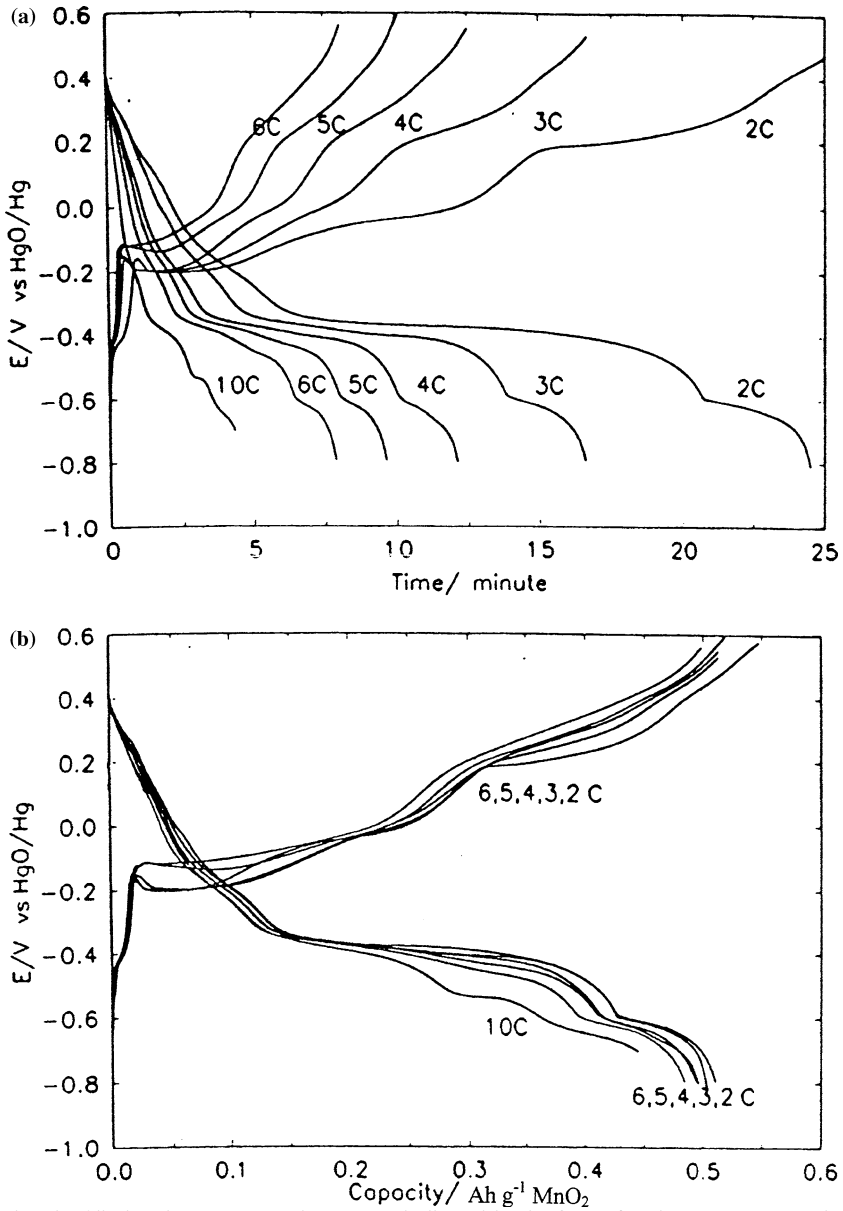

Fig. 5. Constant-current charging/discharging curves at the C rates indicated in the figure for the CM MnO_2 cathode (MnO_2:graphite = 1:10 weight ratio): (a) E vs time; (b) E vs capacity (Ah g^{-1} of MnO_2). The theoretical two-electron capacity for CM MnO_2 is 0.6167 Ah g^{-1}. 2C, 3C, 4C, 5C and 10C rates are equivalent to 1.2, 1.8, 2.5, 3, 3.7 and 6.2 A g^{-1}, respectively.

Kinetically, the Faradaic polarization depends on the activation energy for the charge-transfer process. For non-doped MnO_2, the charge transfer for the second electron can only take place at very low potential (−0.85 V vs HgO/Hg) and at very low rate [1]. The overpotential for the second electron is significantly reduced, while the reduction rate is remarkably increased, with doping by Bi. It appears that Bi acts as a catalyst for the second electron oxidation/reduction of MnO_2, the activation energy associated with the processes being significantly reduced. Practically, the Faradaic resistance is the rate-determining factor for the reduction of EMD which limits the high-rate application of MnO_2/Zn cells. Bi-doping offers a new opportunity for the improvement of the rate capability for MnO_2 cathodes. It should be emphasized that, generally, Bi-doping can significantly improve rate capability of MnO_2 due to the facts [10, 11] that the rate-limiting solid state proton diffusion step is by-passed by the mechanism involving soluble Mn species and the activation energy for the second electron reduction is significantly reduced.

3.3. *Bi-doped MnO_2 synthesized by the CMD method*

CMD is manufactured commercially by the oxidation of Mn^{2+} in the solution to MnO_2 with strong oxidants, e.g. $Na_2S_2O_8$ or $Na_2Cr_2O_7$. The reaction takes place in an homogeneous manner, the MnO_2 being produced is then in its γ-structure. Welsh [20] and Wang et al. [21] disclosed a method for making CMD with fine EMD suspended in the solution. There are two advantages of the process: first, the EMD particles in the reaction solution act both as a

catalyst and as nucleation sites for the formation of CMD. The growth of CMD MnO_2 takes place on the surface of the EMD seeds along the orientation of the EMD crystal structure. Second, the surfaces of MnO_2 particles become rougher, which increases the electrochemical interface area between the MnO_2 particles and the electrolyte, thus enhancing the rate capability of the material.

In order to obtain the required high bulk density and a sufficiently oxidized Bi-doped MnO_2, the CMD process was adopted. The reaction solution contains $MnSO_4$, $Bi(NO_3)_3$ and oxidants; in this case, $Na_2S_2O_8$ was used as oxidant. Fine particle sized EMD ($\leq 10\,\mu m$), obtained by ball milling and screening Kerr-McGee EMD, was used as the seed for the nucleation. As the reaction proceeded, Bi-doped MnO_2 was deposited on the fine EMD surface. The reaction can be represented by:

$$MnSO_4 + Bi(NO_3)_3 + Na_2S_2O_8 + H_2O \rightarrow MnO_2 \cdot Bi_2O_3 + Na_2SO_4 + NaNO_3 \quad (1)$$

Figure 6 shows the X-ray diffraction diagram for the Bi-doped MnO_2 in comparison with that for the EMD seeds. It is obvious that the basic structure of the Bi-doped MnO_2 was still in its gamma form. The arrows in Figure 6 point to the peaks that do not belong to the EMD family. Table 1 tabulates the detailed index and peak positions of the EMD seeds and the Bi-doped EMD. Matching searches were carried out and the identified possible Bi-MnO_2 compounds and their peak indices are also included in Table 1 for comparison.

Most of the MnO_2 deposited on the surface of the EMD seeds still inherits the gamma-like structure; thus its five diffraction peaks are clearly demonstrated in the XRD profile. However, more complex Bi–Mn–O compounds are evidently also formed. It was demonstrated in our previous *in-situ* X-ray absorption work [9], that Bi–O species could be weakly associated with the MnO_2 structure. The Bi–Mn interaction can be detected and the local co-ordination disorder generated by the presence of Bi in the Mn oxide structure was indicated. The XRD results shown in Figure 6 suggest the existence of reasonablely well crystallized Bi–Mn–O compounds. Although Bi_2O_3 may still remain, the two most probable Bi–Mn–O compounds, identified from the XRD by the matching searches, which results are tabulated in Table 1, were $Bi_{7.72}Mn_{0.28}O_{12.14}$ (β-bismuth manganese dioxide) and $Bi_{12}MnO_{20}$ (γ-bismuth manganese dioxide).

The two most intense XRD peaks, which were not associated with MnO_2, are at 27.658 2θ and 28.185 2θ, as shown in Figure 6. It is possible that the two sharp XRD peaks are associated with monoclinic Bi_2O_3, which has two peaks at 27.386 and 28.009, respectively. However, Bi_2O_3 should also have strong peaks at 2θ 25.757, 26.905, 33.026 and 33.228, but these peaks can hardly be identified in the XRD profile in Figure 5; thus the majority compounds formed on the surface of the seed EMD may not be Bi_2O_3.

Bismuth manganese dioxide has two structures, β- and γ-forms. γ-bismuth manganese dioxide has its strongest diffraction peak at 27.525 2θ, while β-bismuth manganese dioxide's strongest diffraction peak is at 27.973. These two diffraction peaks match the two strong and sharp peaks at 27.66 and 28.19 in Figure 6, respectively. Both bismuth manganese dioxides match the position of the rest of the diffraction peaks of Bi-doped MnO_2 very well. Thus, it is reasonable to assume that the bismuth manganese dioxide is formed in the matrix of the CMD, which is deposited on the surface of the EMD seeds.

Figure 4 shows a comparison of the electrochemical discharge curves for the Bi-doped MnO_2 synthesized by three different methods, while Figure 7 shows a com-

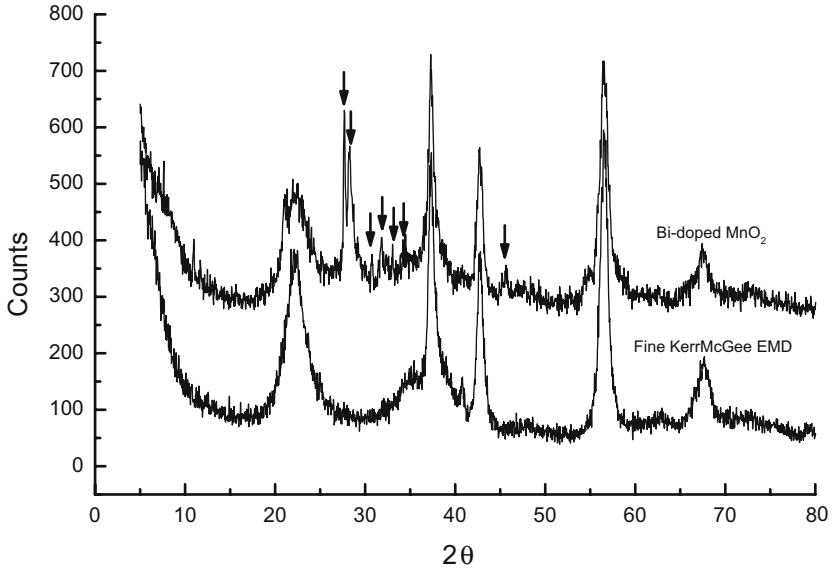

Fig. 6. Comparison of the XRD profiles of Bi-doped MnO_2 made by the CMD method and Kerr-McGee EMD used as seed. The arrows show the diffraction peaks which are not in the family of the EMD material.

Table 1. Line positions and indices for EMD, Bi-doped MnO_2 made using the CMD process, compared with data for Bi_2O_3 and two bismuth manganese dioxide compounds

EMD Seed	Bi-CMD	Bi_2O_3		$Bi_{7.72}Mn_{0.28}O_{12.14}$ β-Bismuth Manganese dioxide		$Bi_{12}MnO_{20}$ γ-Bismuth Manganese Dioxide	
2θ	2θ	2θ	Relative intensity (%)	2θ	Relative intensity (%)	2θ	Relative intensity (%)
	21.024						
22.2	22.279						
						24.62	23
		25.757	23				
		26.905	30				
		27.386	100				
	27.658					27.582	100
				27.973	100		
	28.185	28.009	24				
	29.716						
						30.272	23
	31.774			31.727	25		
	32.464			32.753	44	32.761	72
		33.026	31				
		33.228	36				
34.7	34.611						
	37.282						
37.308							
	37.536						
38.69							
42.737	42.7						
	45.294						
	45.595						
	46.943			46.233	27		
48.091							
	48.444						
	48.562						
	52.734					52.151	34
				54.231	17		
				55.585	29	55.374	24
	55.197						
56.5	56.486						
	57.745						
62.44							

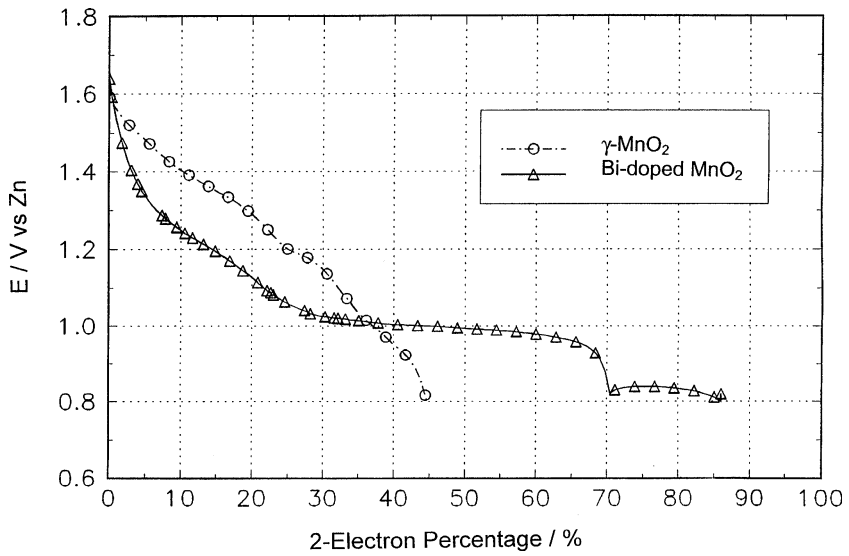

Fig. 7. Comparison of the discharge curves with those for the electrode made with EMD and Bi-doped MnO_2 from the CMD process. The electrodes were discharged at 30.8 mA g^{-1}.

parison of the discharge curves for the Bi-doped MnO_2 made by the CMD method, and the Kerr-McGee EMD. It is clear that the Bi-doped MnO_2 which has gamma-structure demonstrated a higher, EMD-like discharge potential at the early stage of the discharge (discharge curve c in Figure 4). As discussed in earlier publications [e.g. Ref. 22], the Bi only catalyzes the second electron reduction stage through the mechanism involving soluble Mn species. The first part of the discharge curve of the Bi-doped electrode was similar to that of EMD, which has initially high discharge potential; while the second-electron reduction stage commences at −0.9–1.0 V vs Zn as reference electrode.

3.4. *LR06 (AA) primary alkaline MnO_2/Zn cell made with Bi-doped MnO_2 as the cathode*

LR06 type (AA size) cells were made using Bi-doped MnO_2 (CMD) as cathode using the technique referred to in the experimental section. A typical discharge curve of the AA cell is shown in Figure 8 in comparison with that for the commercial AA cell purchased from the open market and AA cell made in-house using Kerr-McGee EMD, as indicated earlier. In comparison with the profile of the discharge curves, the advantage of the cells using Bi-doped MnO_2 is clearly demonstrated. Even though the Bi-doped MnO_2 had lower initial discharge voltage (although above 1.15 V), it exhibited a flatter discharge curve than that of regular EMD throughout the remaining operational voltage range to 0.8 V. The improvement in the performance toward the end of the first electron reduction as compared to the Eveready AA cell may result from the characteristic of the material used and different aging times. We suspect that some of the second electron capacity already becomes utilized in the voltage range of 1.0–0.8 V; of course, the majority of the second-electron charge is released below 0.8 V.

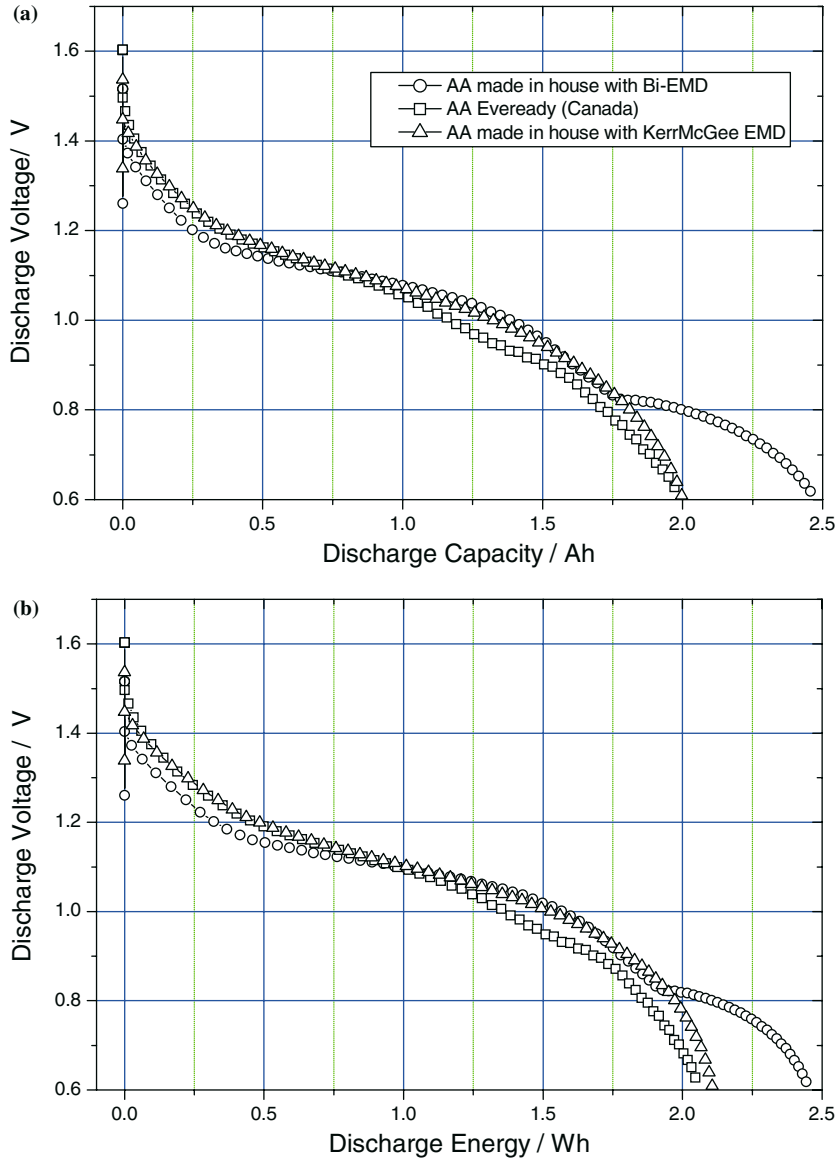

Fig. 8. Comparison of the discharge curves for the Eveready AA cells bought in the open market and the AA cell made in-house with Bi-doped MnO_2 from the CMD process (compare with Figure 3). The cells were discharged through a 5 ohm constant load.

4. Conclusions

1. Bi can reduce the overpotential for the process of second electron reduction of the MnO_2.
2. The Bi-doped MnO_2 needs to be fully oxidized during its synthesis in order to achieve high capacity and high voltage on the very first discharge.
3. The state of the Bi was identified to be that in the form of bismuth manganese dioxide, which stays in the matrix of the Bi-doped MnO_2 made by the CMD process.
4. The major part of the bismuth-enhanced, second-electron stage of MnO_2 reduction arises at relatively low voltage, which is a practical disadvantage.
5. It is, however, feasible to use Bi-doped MnO_2 as a primary alkaline cell cathode, which can provide higher capacity than regular EMD. The performance of Bi-doped MnO_2 could be further improved by the full utilization of the 2 electrons implicit in the overall reduction process on discharge.

References

1. J. McBreen, *Power Sources* **5** (1995) 325.
2. A. Kozawa and J.F. Yeager, *J. Electrochem. Soc.* **115** (1968) 1003.
3. A. Kozawa and R.A. Powers, *J. Electrochem. Soc.* **113** (1966) 870.
4. A. Kozawa and R.A. Powers, *Electrochem. Technol.* **5** (1967) 535.
5. A. Kozawa and R.A. Powers, *J. Electrochem. Soc.* **115** (1968) 122.
6. Y.F. Yao, N. Gupta and H.S. Wroblowa, *J. Electrochem. Soc.* **135** (1987) 107.
7. Y.F. Yao, N. Gopta and H.S. Wroblowa, *J. Electroanal. Chem.* **107** (1987) 223.
8. S. Donne, M. Devernney and A. Gover, WO 01/93348 A2.
9. JA0041846.
10. D.Y. Qu, B.E. Conway, L. Bai, Y.H. Zhou and W.A. Adams, *J. Applied. Electrochem.* **23** (1993) 693.
11. L. Bai, D.Y. Qu, B.E. Conway, T.H. Zhou, G. Chowdhury and W.A. Adams, *J. Electrochem. Soc.* **140** (1993) 884.
12. B.E. Conway, D.Y. Qu and J. McBreen, in C.A. Melendre, A. Tajeddine, (Eds), Synchrotron Techniques in Interfacial Electrochemistry, (Kluwer Academic, Amsterdam, 1994), pp. 311–344.
13. D.Y. Qu, L. Bai, C.G. Castledine, B.E. Conway and W.A. Adams, *J. Electroanal. Chem.* **365** (1994) 247.
14. L.J. Bai, W.A. Adams, B.E. Conway and D.Y. Qu, USP 5,660,953.
15. D.Y. Qu, *Electrochim. Acta* **48** (2003) 1675.
16. Y.F. Yao, USP 4,520,005.
17. D.Y. Qu, US patent publication 2003/0049531 A1.
18. C. Castledine and B.E. Conway, *J Appl. Electrochem.* **25** (1995) 707.
19. J. Zhang, USP 5,250,374.
20. J.Y. Welsh, USP 2,956,860.
21. E.I. Wang, L. Lin and W.L. Bowden, USP 5,348726.
22. D.Y. Qu, *J. Appl. Electrochem.* **29** (1999) 511.